

Solitary wave simulations of the Boussinesq Systems

Ozlem Ersoy^{*,1}, Idiris Dağ¹, and Alper Korkmaz²

¹Department of Mathematics-Computer, Eskişehir Osmangazi University, 26480, Eskişehir, Turkey.

²Department of Mathematics, Çankırı Karatekin University, 18200, Çankırı, Turkey.

May 18, 2016

Abstract

In the study, the collocation method based on exponential cubic B-spline functions is proposed to solve one dimensional Boussinesq systems numerically. Two initial boundary value problems for Regularized and Classical Boussinesq systems modeling motion of traveling waves are considered. The accuracy of the method is validated by measuring the error between the numerical and analytical solutions. The numerical solutions obtained by various values of free parameter p are compared with some solutions in literature.

Keywords: Boussinesq sytems; solitary waves; exponential cubic B-spline; collocation.

MSC2010: 35Q99;35C07;76B25;65D07;65M70.

1 Boussinesq Systems

In the light of the d' Alembert solution, describing two distinct waves moving in the opposite directions for the Cauchy problem for one dimensional wave equation, many physical problems modeled by linear and nonlinear partial differential equations have been solved in wave forms covering traveling waves, solitary waves, harmonic waves, etc. Waves are an important solution class for the model problems in physics, chemistry, and many fields of engineering. This solution type is widely constructed for different models in various media covering solids and fluids. Class of surface bell-shaped solitary waves, having long amplitude when compared with its width, is one of the most prominent classes of waves. In addition to linear equations, solitary wave solutions have also been studied for well known nonlinear equations and systems such as Korteweg-deVries(KdV), Schrödinger, Boussinesq, etc. Having analytical solutions only for some particular cases including additional restrictions and conditions, many numerical methods have been developed to obtain solutions for nonlinear problems.

Dougalis et al. [1] studied the numerical behavior of solitary waves of a member of Boussinesq systems family (Bona-Smith system). In that study, long time stability and possible blow-up solutions were examined under small and large perturbations covering perturbation of amplitudes, system coefficients, etc. Numerical models were constructed with the Galerkin-finite element method on the space S_h of smooth, periodic, cubic splines.

Quintic B-spline collocation technique based on Crank-Nicolson formulation was set up for numerical solutions of Boussines type coupled-BBM system [2]. Two initial boundary value problems describing motion of single solitary wave and interaction of solitary waves were simulated by the proposed method. The numerical results were compared with the analytical ones.

^{*}Ozlem Ersoy, Telephone: +90 222 2393750, Fax: +90 222 2393578, E-mail:ozersoy@ogu.edu.tr

The Galerkin-finite element periodic B-spline method was used to approximate the cnoidal and solitary wave solutions of periodic initial value problem for four variable Boussinesq system [3].

In the study [4], variations of Boussinesq system, namely coupled Korteweg-de Vries (KdV) systems in Hamiltonian form, were integrated using the energy preserving average vector field scheme. The travelling waves for the KdV-KdV systems were also studied numerically by Bona et al. using unconditionally stable periodic splines Galerkin method with Gauss-Legendre implicit Runge-Kutta method of stage two [5].

Antonopoulos et al. simulated the numerical solutions of three initial boundary value problems one parameter Bona-Smith systems [6]. The problems with homogenous Dirichlet, reflection, and periodic boundary conditions were integrated by Galerkin-finite element combined with fourth order explicit Runge-Kutta method.

A meshless radial basis collocation algorithm was set up to simulate nonlinear dispersive waves propagating in two ways of Boussinesq system by Suárez and Morales [7]. The solutions for three initial boundary value problems modeling motion of single solitary and interaction of solitary waves were demonstrated with the proposed method.

Aksoy presented Taylor-Collocation extended cubic B-spline methods for the numerical solutions of the Boussinesq systems [19]. The initial boundary value problems modeling motion of single solitary waves were investigated by using various free parameters in extended cubic B-spline functions.

In this study, the authors investigate the numerical solutions for two particular initial boundary value problems for the Classical Boussinesq System (CBS) and the Regularized Boussinesq System (RBS). A collocation method based on exponential cubic B-spline functions is constructed to obtain the numerical solutions for both systems. The details of both problems and numerical methodology will be explained in the following sections.

Consider the Boussinesq system modeling bi-directional propagation of nonlinear dispersive long surface waves with small amplitudes in a channel of the form

$$\begin{aligned} V_t + U_x + (VU)_x + s_1 U_{xxx} - s_2 V_{xxt} &= 0 \\ U_t + V_x + UU_x + s_3 V_{xxx} - s_4 U_{xxt} &= 0 \end{aligned} \quad (1)$$

where x denotes the distance along the channel scaled by still water of depth h_0 and t is the time scaled by $\sqrt{\frac{h_0}{g}}$, with the gravitational acceleration g [8, 9]. In order to equalize the order of the effects of both nonlinearity and dispersion, the Stokes number $S = s_1 \lambda^2 / h_0^3$ is assumed of order one with the small maximum deviation of surface s_1 relative to h_0 and $\lambda > h_0$. In the model (1), $V(x, t)$ is the scaled, dimensionless deviation of the water surface, $U(x, t)$ is the scaled, dimensionless horizontal velocity of height θh_0 , $\theta \in [0, 1]$ above the bottom of the channel [9]. In the system (1), the real constants s_1, s_2, s_3 and s_4 are defined by;

$$\begin{aligned} s_1 &= \frac{1}{2}(\theta^2 - \frac{1}{3})\lambda \\ s_2 &= \frac{1}{2}(\theta^2 - \frac{1}{3})(1 - \lambda) \\ s_3 &= \frac{1}{2}(1 - \theta^2)\mu \\ s_4 &= \frac{1}{2}(1 - \theta^2)(1 - \mu) \end{aligned} \quad (2)$$

where λ and μ are real [8, 10, 11].

Particular choice of the parameters $\theta^2 = \frac{1}{3}, \mu = 0$ and arbitrary λ generates the CBS from the system (1) [9, 10, 12] as;

$$\begin{aligned} V_t + U_x + (VU)_x &= 0 \\ U_t + V_x + UU_x - \frac{1}{3}U_{xxt} &= 0 \end{aligned} \quad (3)$$

When the parameters are chosen as $\theta^2 = \frac{2}{3}, \lambda = 0, \mu = 0$, the Boussinesq system (1) reduces to the RBS

of the form [11];

$$\begin{aligned} V_t + U_x + (VU)_x - \frac{1}{6}V_{xxt} &= 0 \\ U_t + V_x + UU_x - \frac{1}{6}U_{xxt} &= 0 \end{aligned} \quad (4)$$

Theorem. *Solitary wave solutions for the Boussinesq system (1) is given as;*

$$\begin{aligned} V(x, t) &= V_0 \operatorname{sech}^2(\lambda(x + x_0 - C_s t)) \\ U(x, t) &= \pm \sqrt{\frac{3}{V_0 + 3}} V_0 \operatorname{sech}^2(\lambda(x + x_0 - C_s t)) \end{aligned} \quad (5)$$

where

$$C_s = \frac{3 + 2V_0}{\pm \sqrt{3(3 + V_0)}}, \quad \lambda = \frac{1}{2} \sqrt{\frac{2V_0}{3(s_1 - s_2) + 2s_2(V_0 + 3)}}$$

and V_0 can be any constant satisfying,

- i. $V_0 = \frac{3(1 - 2\kappa)}{2\kappa}$ when $s_1 - s_2 + 2s_4 \neq 0$, $\kappa = \frac{-s_2 + s_3 + 2s_4}{s_1 - s_2 + 2s_4} > 0$ and $(\kappa - 1/2)[(s_2 - s_1)\kappa - s_2] > 0$
- ii. $0 < V_0 < \infty$ when $s_1 = s_2 = s_3 > 0$, $s_4 = 0$
- iii. $-3 \leq V_0 < 0$ when $s_1 = s_2 = s_3 < 0$, $s_4 = 0$
- iv. $V_0 > -3$ and $\frac{3}{V_0 + 3} \notin \left[1, \frac{s_2}{s_4}\right]$ when $s_1 - s_2 + s_4 = 0$, $s_1 = s_3$, $s_4 > 0$
- v. $V_0 > -3$ and $\frac{3}{V_0 + 3} \in \left[1, \frac{s_2}{s_4}\right]$ when $s_1 - s_2 + s_4 = 0$, $s_1 = s_3$, $s_4 < 0$

It should be noted that the constants V_0 and $\pm \sqrt{\frac{3}{V_0 + 3}}V_0$ denote the amplitudes of solitary waves and the constant C_s denotes the velocity of solitary waves in the analytical solution given above [13].

Numerical solutions will be obtained for both initial boundary value problems with the homogenous Neumann boundary conditions at both ends

$$\begin{aligned} \left. \frac{\partial V(x, t)}{\partial x} \right|_{x=a} &= 0, \quad \left. \frac{\partial V(x, t)}{\partial x} \right|_{x=b} = 0, \quad t \geq 0 \\ \left. \frac{\partial U(x, t)}{\partial x} \right|_{x=a} &= 0, \quad \left. \frac{\partial U(x, t)}{\partial x} \right|_{x=b} = 0, \quad t \geq 0 \end{aligned} \quad (6)$$

over the finite problem interval $[a, b]$ are combined with both the CBS and the RBS. The initial conditions for both problems will be chosen in the following sections.

2 Exponential Cubic B-spline Collocation Method(ECC)

Let π be a uniformly distributed grids of the finite interval $[a, b]$, such as,

$$\pi : x_m = a + mh, m = 0, 1, \dots, N$$

where $h = \frac{b-a}{N}$. Then, the exponential cubic B-splines are defined as;

$$B_m(x) = \begin{cases} b_2 \left((x_{m-2} - x) - \frac{1}{\zeta} \sinh(\zeta(x_{m-2} - x)) \right) & , \quad [x_{m-2}, x_{m-1}] \\ a_1 + b_1(x_m - x) + c_1 \exp(\zeta(x_m - x)) + d_1 \exp(-\zeta(x_m - x)) & , \quad [x_{m-1}, x_m] \\ a_1 + b_1(x - x_m) + c_1 \exp(\zeta(x - x_m)) + d_1 \exp(-\zeta(x - x_m)) & , \quad [x_m, x_{m+1}] \\ b_2 \left((x - x_{m+2}) - \frac{1}{\zeta} \sinh(\zeta(x - x_{m+2})) \right) & , \quad [x_{m+1}, x_{m+2}] \\ 0 & , \quad \text{otherwise} \end{cases} \quad (7)$$

where

$$\begin{aligned}
a_1 &= \frac{\zeta h \cosh(\zeta h)}{\zeta h \cosh(\zeta h) - \sinh(\zeta h)}, \\
b_1 &= \frac{\zeta}{2} \frac{\cosh(\zeta h)(\cosh(\zeta h) - 1) + \sinh^2(\zeta h)}{(\zeta h \cosh(\zeta h) - \sinh(\zeta h))(1 - \cosh(\zeta h))}, \\
b_2 &= \frac{2(\zeta h \cosh(\zeta h) - \sinh(\zeta h))}{\zeta}, \\
c_1 &= \frac{1}{4} \frac{\exp(-\zeta h)(1 - \cosh(\zeta h)) + \sinh(\zeta h)(\exp(-\zeta h) - 1)}{(\zeta h \cosh(\zeta h) - \sinh(\zeta h))(1 - \cosh(\zeta h))}, \\
d_1 &= \frac{1}{4} \frac{\exp(\zeta h)(\cosh(\zeta h) - 1) + \sinh(\zeta h)(\exp(\zeta h) - 1)}{(\zeta h \cosh(\zeta h) - \sinh(\zeta h))(1 - \cosh(\zeta h))},
\end{aligned}$$

where ζ is a real parameter [14]. Each exponential cubic B-spline $B_m(x)$ has two continuous principle derivatives defined in the interval $[x_{m-1}, x_{m+2}]$ and $B_m(x)$ itself and its two principle derivatives vanish out of this interval. The set $\{B_{-1}(x), B_0(x), \dots, B_{N+1}(x)\}$ constitutes a basis for the functions defined over the interval $[a, b]$. Since introduced by McCartin, exponential cubic B-spline functions have been used to solve some engineering and physics problems numerically [15–17].

3 Numerical Approximation

Let $U(x, t)$ and $V(x, t)$ be two approximate solutions defined by;

$$U(x, t) \cong \sum_{m=-1}^{N+1} \delta_m B_m(x) \quad (8a)$$

$$V(x, t) \cong \sum_{m=-1}^{N+1} \phi_m B_m(x) \quad (8b)$$

where δ_m and ϕ_m are parameters dependent on time variable. Those parameters will be determined by the collocation method. Then, the two principle derivatives of $U(x, t)$ and $V(x, t)$ are;

$$U'(x, t) \cong \sum_{m=-1}^{N+1} \delta_m B'_m(x) \quad (9a)$$

$$U''(x, t) \cong \sum_{m=-1}^{N+1} \delta_m B''_m(x) \quad (9b)$$

$$V'(x, t) \cong \sum_{m=-1}^{N+1} \phi_m B'_m(x) \quad (9c)$$

$$V''(x, t) \cong \sum_{m=-1}^{N+1} \phi_m B''_m(x) \quad (9d)$$

Using Eq. (8a)-(9d), the approximate nodal values of the functions $U(x, t)$ and $V(x, t)$ and their two principle derivatives are calculated as;

$$\begin{aligned}
U_m &= U(x_m, t) \cong \frac{\sinh(\zeta h) - \zeta h}{2(\zeta h \cosh(\zeta h) - \sinh(\zeta h))} \delta_{m-1} + \delta_m + \frac{\sinh(\zeta h) - \zeta h}{2(\zeta h \cosh(\zeta h) - \sinh(\zeta h))} \delta_{m+1} \\
U'_m &= U'(x_m, t) \cong \frac{\zeta(1 - \cosh(\zeta h))}{2(\zeta h \cosh(\zeta h) - \sinh(\zeta h))} \delta_{m-1} + \frac{\zeta(\cosh(\zeta h) - 1)}{2(\zeta h \cosh(\zeta h) - \sinh(\zeta h))} \delta_{m+1} \\
U''_m &= U''(x_m, t) \cong \frac{\zeta^2 \sinh(\zeta h)}{2(\zeta h \cosh(\zeta h) - \sinh(\zeta h))} \delta_{m-1} - \frac{\zeta^2 \sinh(\zeta h)}{\zeta h \cosh(\zeta h) - \sinh(\zeta h)} \delta_m + \frac{\zeta^2 \sinh(\zeta h)}{2(\zeta h \cosh(\zeta h) - \sinh(\zeta h))} \delta_{m+1} \\
V_m &= V(x_m, t) \cong \frac{\sinh(\zeta h) - \zeta h}{2(p h \cosh(\zeta h) - \sinh(\zeta h))} \phi_{m-1} + \phi_m + \frac{\sinh(\zeta h) - \zeta h}{2(\zeta h \cosh(\zeta h) - \sinh(\zeta h))} \phi_{m+1} \\
V'_m &= V'(x_m, t) \cong \frac{\zeta(1 - \cosh(\zeta h))}{2(\zeta h \cosh(\zeta h) - \sinh(\zeta h))} \phi_{m-1} + \frac{\zeta(\cosh(\zeta h) - 1)}{2(\zeta h \cosh(\zeta h) - \sinh(\zeta h))} \phi_{m+1} \\
V''_m &= V''(x_m, t) \cong \frac{\zeta^2 \sinh(\zeta h)}{2(\zeta h \cosh(\zeta h) - \sinh(\zeta h))} \phi_{m-1} - \frac{\zeta^2 \sinh(\zeta h)}{\zeta h \cosh(\zeta h) - \sinh(\zeta h)} \phi_m + \frac{\zeta^2 \sinh(\zeta h)}{2(\zeta h \cosh(\zeta h) - \sinh(\zeta h))} \phi_{m+1}
\end{aligned} \tag{10}$$

4 Discretization of the Boussinesq System

Under the assumption $s_1 = s_3 = 0$, substituting finite difference approximations into the terms containing the derivatives with respect to the time variable t and Crank-Nicolson approximations instead of the remaining terms reduces the Boussinesq system to;

$$\begin{aligned}
\frac{V^{n+1} - V^n}{\Delta t} + \frac{U_x^{n+1} + U_x^n}{2} + \frac{(VU)_x^{n+1} + (VU)_x^n}{2} - s_2 \frac{V_{xx}^{n+1} - V_{xx}^n}{\Delta t} &= 0 \\
\frac{U^{n+1} - U^n}{\Delta t} + \frac{V_x^{n+1} + V_x^n}{2} + \frac{(UU)_x^{n+1} + (UU)_x^n}{2} - s_4 \frac{U_{xx}^{n+1} - U_{xx}^n}{\Delta t} &= 0
\end{aligned} \tag{11}$$

where $U^{n+1} = U(x, t_n + \Delta t)$ and $V^{n+1} = V(x, t_n + \Delta t)$. The nonlinear terms $(VU)_x^{n+1}$ and $(UU)_x^{n+1}$ are linearized by using Rubin&Gravis' technique [18] as;

$$\begin{aligned}
(VU)_x^{n+1} &\cong (V_x U)^{n+1} + (V U_x)^{n+1} \cong V_x^{n+1} U^n + V_x^n U^{n+1} - V_x^n U^n + V^{n+1} U_x^n + V^n U_x^{n+1} - V^n U_x^n \\
(UU)_x^{n+1} &\cong U^{n+1} U_x^n + U^n U_x^{n+1} - U^n U_x^n
\end{aligned} \tag{12}$$

After linearization of system (11), the approximates (8a), (8b) and (10) to the functions and derivatives are substituted into the linearized form of the system. The resulting equation system are obtained at each grid point as;

$$\begin{aligned}
&\nu_{m1} \delta_{m-1}^{n+1} + \nu_{m2} \phi_{m-1}^{n+1} + \nu_{m3} \delta_m^{n+1} + \nu_{m4} \phi_m^{n+1} + \nu_{m5} \delta_{m+1}^{n+1} + \nu_{m6} \phi_{m+1}^{n+1} \\
&= \nu_{m7} \delta_{m-1}^n + \nu_{m8} \phi_{m-1}^n + \nu_{m9} \delta_m^n + \nu_{m10} \phi_m^n + \nu_{m11} \delta_{m+1}^n + \nu_{m12} \phi_{m+1}^n
\end{aligned} \tag{13}$$

and

$$\begin{aligned}
&\nu_{m12} \delta_{m-1}^{n+1} + \nu_{m13} \phi_{m-1}^{n+1} + \nu_{m14} \delta_m^{n+1} + \nu_{m15} \phi_m^{n+1} + \nu_{m16} \delta_{m+1}^{n+1} + \nu_{m17} \phi_{m+1}^{n+1} \\
&= \nu_{m18} \delta_{m-1}^n + \nu_{m19} \phi_{m-1}^n + \nu_{m20} \delta_m^n + \nu_{m21} \phi_m^n + \nu_{m22} \delta_{m+1}^n + \nu_{m19} \phi_{m+1}^n
\end{aligned} \tag{14}$$

where

$$\begin{aligned}
\nu_{m1} &= \left(\frac{2}{\Delta t} + K_2 \right) \alpha_1 + K_1 \beta_1 - \frac{2s_4}{\Delta t} \gamma_1, & \nu_{m7} &= \frac{2}{\Delta t} \alpha_1 - \frac{2s_4}{\Delta t} \gamma_1, \\
\nu_{m2} &= \beta_1, & \nu_{m8} &= -\beta_1, \\
\nu_{m3} &= \left(\frac{2}{\Delta t} + K_2 \right) - \frac{2s_4}{\Delta t} \gamma_2, & \nu_{m9} &= \frac{2}{\Delta t} - \frac{2s_4}{\Delta t} \gamma_2, \\
\nu_{m4} &= 0, & \nu_{m10} &= 0, \\
\nu_{m5} &= \left(\frac{2}{\Delta t} + K_2 \right) \alpha_1 - K_1 \beta_1 - \frac{2s_4}{\Delta t} \gamma_1, & \nu_{m11} &= \beta_1, \\
\nu_{m6} &= -\beta_1, \\
\nu_{m12} &= L_2 \alpha_1 + (1 + L_1) \beta_1, & \nu_{m18} &= -\beta_1, \\
\nu_{m13} &= \left(\frac{2}{\Delta t} + K_2 \right) \alpha_1 + K_1 \beta_1 - \frac{2s_2}{\Delta t} \gamma_1, & \nu_{m19} &= \frac{2}{\Delta t} \alpha_1 - \frac{2s_2}{\Delta t} \gamma_1, \\
\nu_{m14} &= L_2, & \nu_{m20} &= 0, \\
\nu_{m15} &= \left(\frac{2}{\Delta t} + K_2 \right) - \frac{2s_2}{\Delta t} \gamma_2, & \nu_{m21} &= \frac{2}{\Delta t} - \frac{2s_2}{\Delta t} \gamma_2, \\
\nu_{m16} &= L_2 \alpha_1 - (1 + L_1) \beta_1, & \nu_{m22} &= \beta_1, \\
\nu_{m17} &= \left(\frac{2}{\Delta t} + K_2 \right) \alpha_1 - K_1 \beta_1 - \frac{2s_2}{\Delta t} \gamma_1,
\end{aligned}$$

with

$$\begin{aligned}
K_1 &= \alpha_1 \delta_{m-1}^n + \delta_m^n + \alpha_1 \delta_{m+1}^n \\
L_1 &= \alpha_1 \phi_{m-1}^n + \phi_m^n + \alpha_1 \phi_{m+1}^n \\
K_2 &= \beta_1 \delta_{m-1}^n - \beta_1 \delta_{m+1}^n \\
L_2 &= \beta_1 \phi_{m-1}^n - \beta_1 \phi_{m+1}^n \\
\alpha_1 &= \frac{\sinh(\zeta h) - \zeta h}{2(\zeta h \cosh(\zeta h) - \sinh(\zeta h))} \\
\beta_1 &= \frac{\zeta(1 - \cosh(\zeta h))}{2(\zeta h \cosh(\zeta h) - \sinh(\zeta h))} \\
\gamma_1 &= \frac{\zeta^2 \sinh(\zeta h)}{2(\zeta h \cosh(\zeta h) - \sinh(\zeta h))} \\
\gamma_2 &= -\frac{\zeta^2 \sinh(\zeta h)}{\zeta h \cosh(\zeta h) - \sinh(\zeta h)}
\end{aligned}$$

The discretized system (13)-(14) is written in matrix notation as;

$$\mathbf{A} \mathbf{x}^{n+1} = \mathbf{B} \mathbf{x}^n \quad (15)$$

where

$$\mathbf{A} = \begin{bmatrix}
\nu_{m1} & \nu_{m2} & \nu_{m3} & \nu_{m4} & \nu_{m5} & \nu_{m6} & & & \\
\nu_{m12} & \nu_{m13} & \nu_{m14} & \nu_{m15} & \nu_{m16} & \nu_{m17} & & & \\
& & \nu_{m1} & \nu_{m2} & \nu_{m3} & \nu_{m4} & \nu_{m5} & \nu_{m6} & \\
& & \nu_{m12} & \nu_{m13} & \nu_{m14} & \nu_{m15} & \nu_{m16} & \nu_{m17} & \\
& & & \ddots & \ddots & \ddots & \ddots & \ddots & \ddots \\
& & & & \nu_{m1} & \nu_{m2} & \nu_{m3} & \nu_{m4} & \nu_{m5} & \nu_{m6} \\
& & & & \nu_{m12} & \nu_{m13} & \nu_{m14} & \nu_{m15} & \nu_{m16} & \nu_{m17}
\end{bmatrix}$$

$$\mathbf{B} = \begin{bmatrix} \nu_{m7} & \nu_{m8} & \nu_{m9} & \nu_{m10} & \nu_{m7} & \nu_{m11} & & & & \\ \nu_{m18} & \nu_{m19} & \nu_{m20} & \nu_{m21} & \nu_{m22} & \nu_{m19} & & & & \\ & & \nu_{m7} & \nu_{m8} & \nu_{m9} & \nu_{m10} & \nu_{m7} & \nu_{m11} & & \\ & & \nu_{m18} & \nu_{m19} & \nu_{m20} & \nu_{m21} & \nu_{m22} & \nu_{m19} & & \\ & & & \ddots & \ddots & \ddots & \ddots & \ddots & \ddots & \\ & & & & \nu_{m7} & \nu_{m8} & \nu_{m9} & \nu_{m10} & \nu_{m7} & \nu_{m11} \\ & & & & \nu_{m18} & \nu_{m19} & \nu_{m20} & \nu_{m21} & \nu_{m22} & \nu_{m19} \end{bmatrix}$$

and

$$\mathbf{x}^{n+1} = [\delta_{-1}^{n+1}, \phi_{-1}^{n+1}, \delta_0^{n+1}, \phi_0^{n+1}, \dots, \delta_{N+1}^{n+1}, \phi_{N+1}^{n+1}]^T$$

The system (15) contains $2N+2$ equations and $2N+6$ unknowns. The homogenous Neumann boundary conditions at both ends $\frac{\partial V(x,t)}{\partial x} \Big|_{x=a} = \frac{\partial V(x,t)}{\partial x} \Big|_{x=b} = \frac{\partial U(x,t)}{\partial x} \Big|_{x=a} = \frac{\partial U(x,t)}{\partial x} \Big|_{x=b}$ are adapted as;

$$\delta_{-1} = \delta_1, \phi_{-1} = \phi_1, \delta_{N+1} = \delta_{N-1}, \phi_{N+1} = \phi_{N-1}$$

in order to convert (15) to a solvable system. The resultant linear equation system is solved using Thomas algorithm.

5 The Initial State

The start vector \mathbf{x}^0 should be obtained in order to be able to start the iteration in (15). Rearranging the initial and boundary conditions

$$\begin{aligned} U^0(x_0, 0) &= \frac{\sinh(\zeta h) - \zeta h}{2(\zeta h \cosh(\zeta h) - \sinh(\zeta h))} \delta_{-1}^0 + \delta_0^0 + \frac{\sinh(\zeta h) - \zeta h}{2(\zeta h \cosh(\zeta h) - \sinh(\zeta h))} \delta_1^0 \\ U^0(x_m, 0) &= \frac{\sinh(\zeta h) - \zeta h}{2(\zeta h \cosh(\zeta h) - \sinh(\zeta h))} \delta_{m-1}^0 + \delta_m^0 + \frac{\sinh(\zeta h) - \zeta h}{2(\zeta h \cosh(\zeta h) - \sinh(\zeta h))} \delta_{m+1}^0, \quad m = 1, 2, \dots, N-1 \\ U^0(x_N, 0) &= U_N^0 = \frac{\sinh(\zeta h) - \zeta h}{2(\zeta h \cosh(\zeta h) - \sinh(\zeta h))} \delta_{N-1}^0 + \delta_N^0 + \frac{\sinh(\zeta h) - \zeta h}{2(\zeta h \cosh(\zeta h) - \sinh(\zeta h))} \delta_{N+1}^0 \end{aligned} \quad (16)$$

and

$$\begin{aligned} V^0(x_0, 0) &= \frac{\sinh(\zeta h) - \zeta h}{2(\zeta h \cosh(\zeta h) - \sinh(\zeta h))} \phi_{-1}^0 + \phi_0^0 + \frac{\sinh(\zeta h) - \zeta h}{2(\zeta h \cosh(\zeta h) - \sinh(\zeta h))} \phi_1^0 \\ V^0(x_m, 0) &= \frac{\sinh(\zeta h) - \zeta h}{2(\zeta h \cosh(\zeta h) - \sinh(\zeta h))} \phi_{m-1}^0 + \phi_m^0 + \frac{\sinh(\zeta h) - \zeta h}{2(\zeta h \cosh(\zeta h) - \sinh(\zeta h))} \phi_{m+1}^0, \quad m = 1, 2, \dots, N-1 \\ V^0(x_N, 0) &= \frac{\sinh(\zeta h) - \zeta h}{2(\zeta h \cosh(\zeta h) - \sinh(\zeta h))} \phi_{N-1}^0 + \phi_N^0 + \frac{\sinh(\zeta h) - \zeta h}{2(\zeta h \cosh(\zeta h) - \sinh(\zeta h))} \phi_{N+1}^0 \end{aligned} \quad (17)$$

gives $N+1$ equations with $N+3$ unknowns. Using

$$\begin{aligned} \delta_{-1}^0 &= \delta_1^0 + \frac{2(\zeta h \cosh(\zeta h) - \sinh(\zeta h))}{\zeta(1 - \cosh(\zeta h))} U'_0 \\ \delta_{N+1}^0 &= \delta_{N-1}^0 - \frac{2(\zeta h \cosh(\zeta h) - \sinh(\zeta h))}{\zeta(1 - \cosh(\zeta h))} U'_N \\ \phi_{-1}^0 &= \phi_1^0 + \frac{2(\zeta \cosh(\zeta h) - \sinh(\zeta h))}{\zeta(1 - \cosh(\zeta h))} V'_0 \\ \phi_{N+1}^0 &= \phi_{N-1}^0 - \frac{2(\zeta \cosh(\zeta h) - \sinh(\zeta h))}{\zeta(1 - \cosh(\zeta h))} V'_N \end{aligned}$$

the parameters $\delta_{-1}^0, \delta_{N+1}^0, \phi_{-1}^0$ and ϕ_{N+1}^0 can be eliminated from the system (16)-(17). The resultant linear equation system;

$$\begin{bmatrix} 1 & \frac{\tilde{s}-\zeta h}{\zeta h \tilde{c}-\tilde{s}} & & & \\ \frac{\tilde{s}-\zeta h}{2(\zeta h \tilde{c}-\tilde{s})} & 1 & \frac{\tilde{s}-\zeta h}{2(\zeta h \tilde{c}-\tilde{s})} & & \\ & & \ddots & & \\ & & & \frac{\tilde{s}-\zeta h}{2(\zeta h \tilde{c}-\tilde{s})} & 1 & \frac{\tilde{s}-\zeta h}{2(\zeta h \tilde{c}-\tilde{s})} \\ & & & \frac{\tilde{s}-\zeta h}{\zeta h \tilde{c}-\tilde{s}} & 1 \end{bmatrix} \begin{bmatrix} \delta_0^0 \\ \delta_1^0 \\ \vdots \\ \delta_{N-1}^0 \\ \delta_N^0 \end{bmatrix} = \begin{bmatrix} U_0 - \frac{\tilde{s}-\zeta h}{\zeta(1-\tilde{c})} U'_0 \\ U'_1 \\ \vdots \\ U'_{N-1} \\ U_N - \frac{\tilde{s}-\zeta h}{\zeta(\tilde{c}-1)} U'_N \end{bmatrix}$$

and

$$\begin{bmatrix} 1 & \frac{\tilde{s}-\zeta h}{\zeta h \tilde{c}-\tilde{s}} & & & \\ \frac{\tilde{s}-\zeta h}{2(\zeta h \tilde{c}-\tilde{s})} & 1 & \frac{\tilde{s}-\zeta h}{2(\zeta h \tilde{c}-\tilde{s})} & & \\ & & \ddots & & \\ & & & \frac{\tilde{s}-\zeta}{2(\zeta h \tilde{c}-\tilde{s})} & 1 & \frac{\tilde{s}-\zeta h}{2(\zeta h \tilde{c}-\tilde{s})} \\ & & & \frac{\tilde{s}-\zeta h}{\zeta h \tilde{c}-\tilde{s}} & 1 \end{bmatrix} \begin{bmatrix} \phi_0^0 \\ \phi_1^0 \\ \vdots \\ \phi_{N-1}^0 \\ \phi_N^0 \end{bmatrix} = \begin{bmatrix} V_0 - \frac{\tilde{s}-\zeta h}{\zeta(1-\tilde{c})} V'_0 \\ V'_1 \\ \vdots \\ V'_{N-1} \\ V_N - \frac{\tilde{s}-\zeta h}{\zeta(\tilde{c}-1)} V'_N \end{bmatrix}$$

where $\tilde{c} = \cosh(\zeta h)$ and $\tilde{s} = \sinh(\zeta h)$ is solved by Thomas algorithm for 3-banded systems to obtain the initial vector \mathbf{x}^0 .

6 Numerical Examples

The accuracy and efficiency of the proposed method will be validated by solving initial boundary value problems for RBS and CBS. The numerical results will be compared with the analytical solutions and the Aksoy's numerical solutions obtained by extended cubic B-spline collocation method (EXCC) with free parameter λ [19]. The error between the numerical solution ψ^{num} and the analytical solution ψ^{ana} at a time t will be measured by using discrete maximum error norm $L_\infty(\psi)$ defined as;

$$L_\infty(\psi) = |\psi^{ana} - \psi^{num}|_\infty = \max_m |\psi_m^{ana} - \psi_m^{num}|$$

6.1 Regularized Boussinesq System

The analytical solution for the RBS is of the form;

$$V(x, t) = -1$$

$$U(x, t) = (1 - \frac{\rho}{6})C_s + \frac{C_s \rho}{2} \text{sech}^2(\frac{\sqrt{\rho}}{2}(x + x_0 - C_s t))$$

where x_0 and C_s real, ρ nonnegative constant [9]. This solution represents a traveling wave, the peak of which is located at x_0 initially, moving along the horizontal axis with velocity C_s . The initial-boundary value problem for the RBS is constructed by combining the initial conditions

$$V(x, 0) = -1$$

$$U(x, 0) = \text{sech}^2(\frac{\sqrt{6}}{2}x) \quad (18)$$

and the homogenous Neumann boundary conditions

$$\left. \frac{\partial U(x, t)}{\partial x} \right|_{x=-20} = 0, \quad \left. \frac{\partial U(x, t)}{\partial x} \right|_{x=30} = 0$$

$$\left. \frac{\partial V(x, t)}{\partial x} \right|_{x=-20} = 0, \quad \left. \frac{\partial V(x, t)}{\partial x} \right|_{x=30} = 0$$

over the finite interval $[-20, 30]$. The initial condition representing a pulse of amplitude 1 is derived from the analytical solution by a particular choice of $x_0 = 0$, $\rho = 6$ and $C_s = 1/3$ at the initial time $t = 0$. The numerical simulation of wave motion along the horizontal axis is accomplished with the parameters $N = 1000$, $\Delta t = 0.005$ and $\zeta = 0.0000058339$ up to the terminating time 15, Fig 1. The peak of the initial pulse moves from its initial location $x_0 = 0$ with a constant velocity $C_s = 1/3$. At the terminating time $t = 15$, the peak reaches $x = 5$ without changing its shape. For the sake of comparison with Aksoy's work,

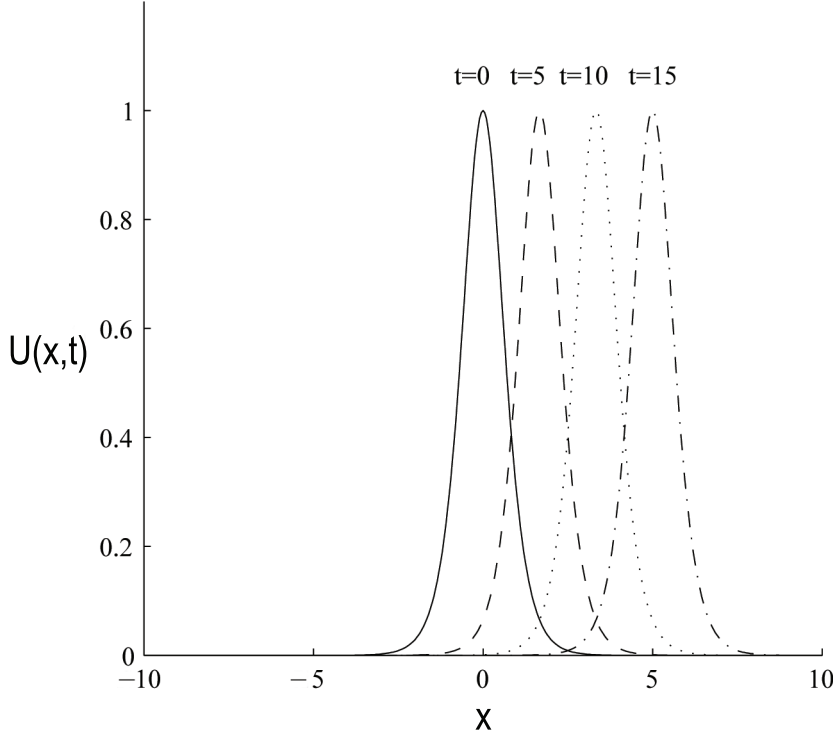
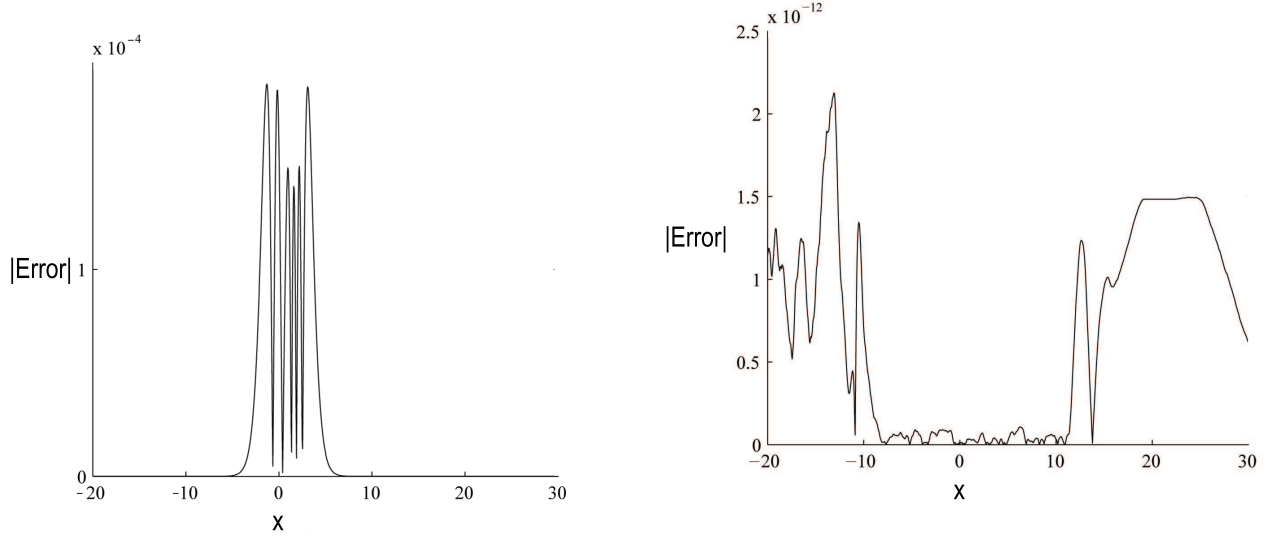


Figure 1: Simulation of wave motion along the horizontal axis

the designed algorithms are run with fixed number grids $N = 1000$, the various parameters ζ and time step lengths. The measured maximum errors for both $U(x, t)$ and $V(x, t)$ at the terminating time $t = 5$ are depicted in Fig 2(a) and Fig 2(b). Even though the maximum error for $U(x, 5)$ is located about the peak, the maximum error for $V(x, 5)$ is about $x = -15$. When ECC is compared with EXCC, one see that ECC generates a little bit better numerical results for both various choices of free parameters. When $\Delta t = 0.005$, the maximum error is approximately 2×10^{-11} for $\lambda = 0$ and 3×10^{-11} for $\lambda = -0.00297$ for the function $V(x, t)$ in EXCC. Usage of the same parameters except λ , the maximum error is measured less than 10^{-11} for various choices of ζ in ECC. For the function $U(x, t)$, the accuracy of the numerical results are in the same digits for both methods for various values of free parameters λ and ζ .

Table 1: Comparison with Aksoy's work ($L_\infty(V) \times 10^5$ at the terminating time $t = 5$)

Δt	EXCC [19] ($\lambda = 0$)	ECC ($\zeta = 1$)	EXCC [19]	ECC
0.5	0.000000	0.000000	0.000000($\lambda = -0.0642$)	0.000000($\zeta = 0.0000018762$)
0.05	0.000000	0.000000	0.000000($\lambda = -0.003627$)	0.000000($\zeta = 0.0000060571$)
0.005	0.000002	0.000000	0.000003($\lambda = -0.00297$)	0.000000($\zeta = 0.0000058339$)



(a) Error distribution for $U(x, t)$ at $t = 5$

(b) Error distribution for $V(x, t)$ at $t = 5$

Figure 2: Error distribution for both $U(x, t)$ and $V(x, t)$ with $\zeta = 0.0000058339$ and $\Delta t = 0.005$

Table 2: Comparison with Aksoy's work ($L_\infty(U) \times 10^3$ at the terminating time $t = 5$)

Δt	EXCC [19] ($\lambda = 0$)	ECC ($\zeta = 1$)	EXCC [19]	ECC
0.5	23.364410	23.890978	4.839046($\lambda = -0.0642$)	2.994220($\zeta = 0.0000018762$)
0.05	1.435993	1.554225	0.439634($\lambda = -0.003627$)	0.186862($\zeta = 0.0000060571$)
0.005	1.231550	1.351017	0.369655($\lambda = -0.00297$)	0.189722($\zeta = 0.0000058339$)

6.2 Classical Boussinesq System (CBS)

The traveling wave solution for CBS is,

$$V(x, t) = -1$$

$$U(x, t) = (1 - \frac{\rho}{3})C_s + \frac{C_s\rho}{2} \operatorname{sech}^2(\frac{\sqrt{\rho}}{2}(x + x_0 - C_s t))$$

where x_0 and C_s are real, ρ is non negative constants [9]. This solution represents a traveling wave along the horizontal axis with velocity C_s as time goes. The initial boundary value problem for CBS is constructed by combining the initial condition

$$V(x, 0) = -1$$

$$U(x, 0) = \operatorname{sech}^2(\frac{\sqrt{3}}{2}x)$$

which is generated by a particular choice of the constants as $x_0 = 0$, $\rho = 3$ and $C_s = 1/3$ at the initial time $t = 0$ in the analytical solution, and the homogenous Neumann boundary conditions covering only first order derivatives at both ends. By those selection of parameters, the analytical solution representing

a traveling wave of amplitude 1 and of initial peak position 0 moves along the horizontal axis with velocity $1/3$ as time goes. The simulation of the numerical solution is depicted with $N = 1000$, $\Delta t = 0.005$ and $\zeta = 0.0000086530$ up to the terminating time $t = 15$, Fig 3. The initial pulse moves along the horizontal axis without changing its shape during the simulation. The peak position becomes $x = t \times C_s = 15 \times \frac{1}{3} = 5$ at the terminating time $t = 15$. The error distribution for both function are graphed with the parameters $N = 1000$, $\Delta t = 0.005$ and $\zeta = 0.0000086530$ at the time $t = 5$ in Fig 4(a)-4(b). The maximum errors are measured about 1×10^{-4} for $U(x, 5)$ and 1×10^{-14} for $V(x, 5)$.

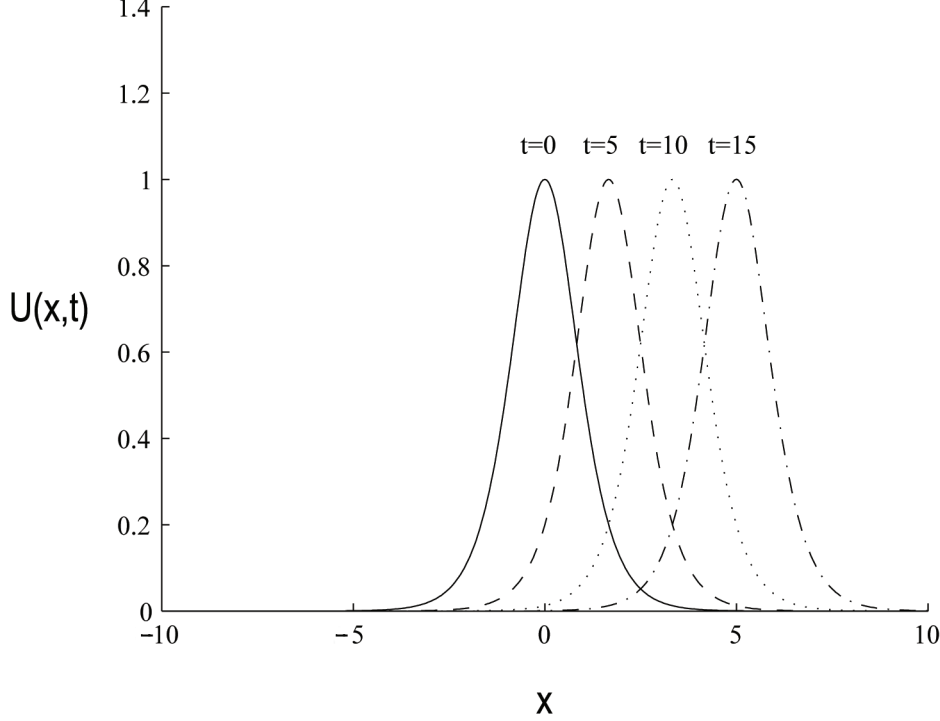
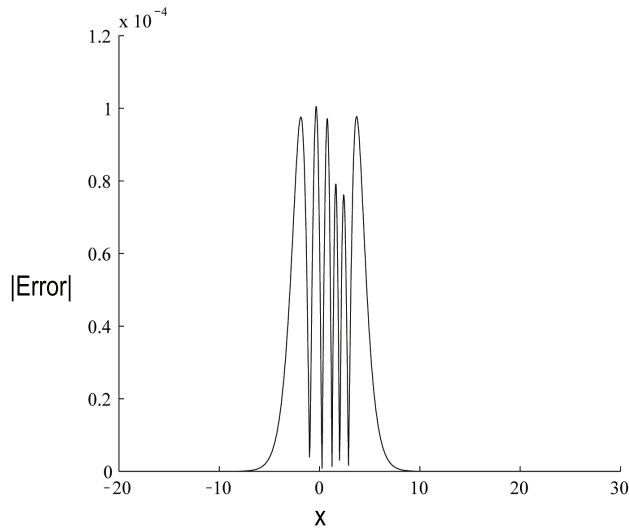


Figure 3: Simulation of traveling wave along the horizontal axis

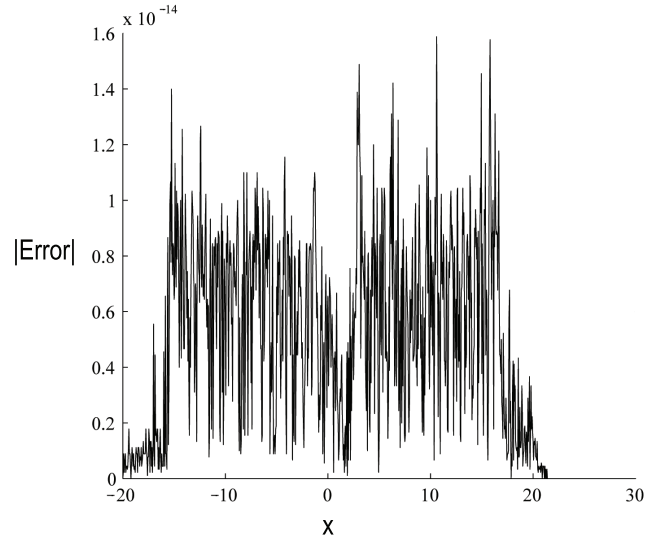
The results are compared with the analytical solutions and Aksoy' s solutions by measuring the error between numerical and analytical solutions for various values of the parameter ζ , Table 3- Table 4. Even though the accuracy of $V(x, t)$ are almost the same in both methods, the accuracy of $U(x, t)$ appears a little bit better for various values of free parameters in ECC.

Table 3: Comparison with Aksoy's work ($L_\infty(V) \times 10^5$ at the terminating time $t = 5$)

Δt	EXCC [19] ($\lambda = 0$)	ECC ($\zeta = 1$)	EXCC [19]	ECC
0.5	0.000000	0.000000	0.000000($\lambda = -0.0332$)	0.000000($\zeta = 0.0000027881$)
0.05	0.000000	0.000000	0.000000($\lambda = -0.00197$)	0.000000($\zeta = 0.0000080030$)
0.005	0.000006	0.000006	0.000000($\lambda = -0.0017$)	0.000000($\zeta = 0.0000086530$)



(a) Error distribution for $U(x, t)$ at $t = 5$



(b) Error distribution for $V(x, t)$ at $t = 5$

Figure 4: Error distribution for both $U(x, t)$ and $V(x, t)$ with $\zeta = 0.0000086530$ and $\Delta t = 0.005$

Table 4: Comparison with Aksoy's work ($L_\infty(U) \times 10^3$ at the terminating time $t = 5$)

Δt	EXCC [19] ($\lambda = 0$)	ECC ($\zeta = 1$)	EXCC [19]	ECC
0.5	9.915176	8.574594	2.279022($\lambda = -0.0339$)	0.199469($\zeta = 0.0000027881$)
0.05	0.631048	0.715209	0.206695($\lambda = -0.00197$)	0.097838($\zeta = 0.0000080030$)
0.005	0.551502	0.643377	0.182177($\lambda = -0.0017$)	0.100474($\zeta = 0.0000086530$)

7 Conclusion

In the study, the exponential cubic B-spline collocation algorithm is designed to solve two initial boundary value problems modeling traveling wave solutions for Regularized Boussinesq and Classical Boussinesq systems. The equations in systems are discretized in time by Crank-Nicolson and finite difference methods. Then, the resultant equations are discretized in space by collocation method based on exponential B-splines. The simulations are obtained successfully by the proposed method.

The error of numerical results is measured using discrete maximum error norm and compared with the results obtained by Aksoy's method based on extended cubic B-splines. The comparison shows that the results obtained by the proposed method in this study generate more accurate results than Aksoy's results for some problems due to the appropriate choice of free parameter ζ . For the remaining problems, the results are acceptable and as accurate as Aksoy's results.

References

- [1] Dougalis, V.A., Duran, A., López-Marcos, M.A., Mitsotakis, D.E., A Numerical Study of the Stability of Solitary Waves of the Bona-Smith Family of Boussinesq Systems, Journal of Nonlinear Science,

17, 569-607, 2007.

- [2] Behzadi S.S., Yildirim A., Application of Quintic B-Spline Collocation Method for Solving the Coupled-BBM System, Middle-East Journal of Scientific Research, 15, 11, 1478-1486, 2013.
- [3] Antonopoulos, D.C., Dougalis V.A., Mitsotakis D.E., Galerkin Approximations of Periodic Solutions of Boussinesq Systems, Bulletin of the Greek Mathematical Society, 57, 13-30, 2010.
- [4] Karasözen B., Şimşek G., Energy preserving integration of KdV-KdV systems, TWMS Journal of Applied and Engineering Mathematics, 2, 2, 219-227, 2012.
- [5] Bona, J.L., Dougalis V.A., Mitsotakis, D.E., Numerical solution of KdV-KdV systems of Boussinesq equations I. The numerical scheme and generalized solitary waves, Mathematics and Computers in Simulation, 74, 214-228, 2007.
- [6] Antonopoulos, D.C., Dougalis V.A., Mitsotakis D.E., Numerical solution of Boussinesq systems of the Bona-Smith family, Applied Numerical Mathematics, 60, 314-336, 2010.
- [7] Suárez P.U., Morales, J.H., Numerical Solutions of Two-Way Propagation of Nonlinear Dispersive Waves Using Radial Basis Functions, International Journal of Partial Differential Equations, Article ID 407387, 1-8, 2014.
- [8] Bona, J.L., Saut, J.-C., Toland, J.F., Boussinesq equations for small-amplitude long wavelength water waves, preprint, 1997.
- [9] Chen, M., Exact traveling-wave solutions to bidirectional wave equations, International Journal of Theoretical Physics, 37, 5, 1547-1567, 1998.
- [10] Bona, J.L., Chen, M., A Boussinesq system for two way propagation of nonlinear dispersive waves, Physica D, 116, 191-224, 1998.
- [11] Bona, J.L., Chen, M., Saut, J.-C., Boussinesq equations and other systems for small-amplitude long waves in nonlinear dispersive media I: derivation and linear theory, Journal of Nonlinear Science, 12, 283-318, 2002.
- [12] Boussinesq, J.V., Théorie de l'intumescence liquide appelée onde solitaire ou de translation se propageant dans un canal rectangulaire, Comptes Rendus de l'Académie de Sciences, 72, 755-759, 1871.
- [13] Chen, M., Exact solutions of various Boussinesq systems, Applied Mathematics Letters, 5, 45-49, 1998.
- [14] McCartin, B.J., Theory of exponential splines, Journal of Approximation Theory, 66, 1, 1-23, 1991.
- [15] Mohammadi, R., Exponential B-Spline Solution of Convection-Diffusion Equations, Applied Mathematics, 4, 933-944, 2013.
- [16] Mohammadi, R., Exponential B-spline collocation method for numerical solution of the generalized regularized long wave equation, Chin. Phys. B, 24, 5, 050206, 2015.
- [17] Ersoy, O., Dag, I., The exponential cubic B-spline algorithm for Korteweg-deVries Equation, Advances in Numerical Analysis, Article ID 367056, 2015.
- [18] Rubin, S. G., Graves, R. A., Cubic spline approximation for problems in fluid mechanics, Nasa TR R-436, Washington DC, 1975.
- [19] Aksoy, A. M., 2012, Numerical Solutions of Some Partial Differential Equations Using the Taylor Collocation-Extended Cubic B-spline Functions, Eskişehir Osmangazi University, Doctoral Dissertation, Eskişehir, 2012.